An analysis of the emergency isolation of high-pressure pipelines transporting supercritical fluids

Sergey Martynov, PhD, Senior Research Associate

Haroun Mahgerefteh, Professor

Jianhao Yu, PhD student

Department of Chemical Engineering, University College London, WC1E 7JE, London, U.K.

Emergency Shutdown Valves (ESDV) represent the front line mitigating measure in the event of the accidental failure of long pipelines transporting pressurised hazardous fluids. In order to select the appropriate ESDV type and its strategic positioning along such pipelines, the decompression flow behaviour during the emergency isolation must be fully understood.

The present study employs a computational fluid dynamics (CFD) model for evaluating the efficacy of several types of ESDVs, including Automatic Shut-off Valves (ASV), Remotely operated Control Valves (RCV) and non-return Check Valves (CV), installed along a 250 mm i.d. buried supercritical ethylene pipeline at a maximum operating pressure of 90 bar and temperatures between 5 ºC and 30 ºC, chosen as a case example. Based on the comparison of the amount of inventory escaping prior to complete valve closure, the simulation results show that installing CVs along the pipeline already equipped with ASVs offers no additional benefits, while combining CVs with RCVs enables faster emergency isolation of the pipeline. Additionally, despite the advantage of rapid closure, it is found that check valves can result in pressure surges as high as 32 bar above the nominal pipeline operating pressure, posing the risk of secondary catastrophic failure of a pipeline. Best practice recommendations for the selection of the appropriate ESDV type and spacing, whilst at the same time ensuring the pipeline's mechanical integrity, are discussed.

Introduction

To date, over 4.4 million km of pipelines have been constructed, representing the most economic and efficient means for long-distance transportation of enormous quantities of hydrocarbons around the world (CIA 2017). In particular, driven by continuous growth in the demand for ethylene as valuable chemical for manufacturing polymers, high-pressure ethylene pipelines and pipeline networks are being developed in various countries (UKOPA 2009; EPPLP 2017; S&P Global 2012; EPS 2013; QNRF 2014). Given the high flammability of ethylene, its pipeline transportation is considered as a major accident hazard (Papadakis 1999), which require using emergency shut-down valves (ESDVs) as a primary measure for rapid isolation of an accidently ruptured section of a pipeline (DOT 2012; UK Gov & HSE 1996). In the turn, choosing the type and strategic positions of ESDVs, requires estimation of the release duration, as the key factor that determines the time for mitigation of the hazardous consequences of pipeline failure (Oland et al. 2012; Woo 2016).

In order to predict accurately the emergency isolation for pipelines transporting compressible fluids, such as supercritical ethylene, mathematical models have been developed accounting for transient pipeline decompression process and the dynamic response of the isolation valves (Mahgerefteh et al. 1997; Vorozhtsov et al. 2008; Sulfredge 2006). In this respect, the important valve-specific characteristics are their activation and response times.

In the case of high-pressure pipelines transporting gases and liquids, the following three main types of ESDVs are used (Oland et al. 2012):

- Automatic Shut-off Valves (ASV) close upon detection of a change in the flow pressure. The ASV activation time is determined by the duration of the fluid decompression at the valve location down to a specified pressure threshold.
- Remotely Controlled Valves (RCV) are equipped with an actuator closing the valve based on a signal from an operator. The RCVs activation time is the sum of the time lapse for detection of the pressure drop at the valve location and the time duration of the operator action.
- Check Valves (CV) are designed to prevent backflow from a downstream section of a pipeline in high-consequence areas, such as water basins and population centres (Oland et al. 2012; DNV 2010). The CV activation happens at the moment of the flow reversal at the valve location.

In comparison with ASVs and RCVs, CVs offer faster cut-off of a backflow upstream of the ruptured section of pipeline (Mahgerefteh et al. 1997). However, selecting CVs requires considering pressure surges (Ord 2006; Goodwin International Ltd 2014), which can develop upon the valve closure as a result of conversion of the flow kinetic energy into pressure, causing noise and vibrations, and potentially damaging the valve and the pipeline (Koetzier 1986).

In engineering approaches, to estimate the magnitude of pressure surges in pipelines, the Joukowsky equation is commonly used (Muhlbauer 2004). This equation becomes particularly useful in applications where the pipeline flow is steady-state, and its velocity is known prior to valve activation. However, in case of emergency isolation of a ruptured section of a pipeline, the flow velocity at the time of valve closure is not known *a priori*. In this case, computational fluid dynamics models can be applied to simulate accurately all features of the flow, including the flow velocity and the pressure surge waves emerging upon the valve activation (Mahgerefteh et al. 1997; Mahgerefteh et al. 2000).

In our previous work a mathematical model predicting the transient flow and the dynamic response of CVs and ball-type ASVs installed in pressurised pipelines was developed (Mahgerefteh et al. 1997; Mahgerefteh et al. 2000) and recently validated against experiments involved in emergency isolation of CO_2 pipelines (Mahgerefteh et al. 2016). These studies showed that the magnitude of pressure surges depend on the CV closure delay time, compressibility and density of the fluid, as well as relative distance between the rupture plane and the valve. Also, it was found that incorporating in the model a real-gas equation of state, accounting for partial condensation of the gas, resulted in weaker pressure surges compared with predictions based on the ideal gas equation of state (Mahgerefteh et al. 2000).

The above studies confirm that the fluid thermodynamic properties may have profound impact on the dynamics of the flow during the pipeline emergency isolation. This particularly applies to high-pressure pipelines transporting ethylene, which properties and decompression scenario can vary significantly with the initial pressure and temperature and the corresponding thermodynamic state. At the moment, however, no studies have examined the impact of transportation conditions on pressure surges in ethylene pipelines.

Also, given that CVs are designed to prevent the backflow, they cannot be considered as the only resort for emergency isolation in long multi-segment pipelines, but should be setup in combination with ASVs or RCVs. This calls for characterisation of efficacy of CVs as auxiliary type of ESDVs in long pipelines.

The present paper is organised as follows. Methodology section describes the models applied to simulate the transient flow in the pipeline, the physical properties of the fluid and the valves dynamics for ASV, RCV and CV valves. Results and Discussion sections covers main findings of the computational studies, including the investigation of pressure surges induced by closure of CVs, and also comparison of efficacy of CVs, RCVs and ASVs for the emergency isolation of high-pressure ethylene pipelines. The last section summarises conclusions for the study.

Methodology

Pipeline decompression model

In the present study, modelling of the dynamic response of valves to accidental failure in a pipeline is performed for a worst-case scenario involving Full-Bore Rupture (FBR) of a pipeline. In this case, the transient flow in a pipeline can be described using a homogeneous equilibrium mixture model, based on the set of one-dimensional conservation equations of mass, momentum and energy (Mahgerefteh et al. 1997):

$$\frac{\partial \rho}{\partial t} + \frac{\partial \rho u}{\partial x} = 0 \tag{1}$$

$$\frac{\partial \rho u}{\partial t} + \frac{\partial (\rho u^2 + p)}{\partial x} = -\frac{f_w \rho u^2}{D} \tag{2}$$

$$\frac{\partial \rho E}{\partial t} + \frac{\partial (\rho u E + u p)}{\partial x} = -\frac{f_w \rho u^3}{D} \tag{3}$$

where ρ, u, E and p are respectively the fluid density, velocity, total specific energy and pressure, x and t are the spatial coordinate and time, D is the pipeline internal diameter and f_w is the Fanning friction factor, which in the present study is calculated using Chen's correlation (Chen 1979).

To enable numerical solution of the above equations, boundary conditions are specified at the upstream and downstream ends of the pipeline. In particular, at the upstream end of the pipe the feed stream boundary condition is applied to simulate the presence of a pump/compressor. At the downstream end of the pipe a zero-gradient boundary condition is applied to simulate the pipeline connection to next segment.

Fluid properties

In order to close the set of equations (1)-(3), correlations for evaluation of fluid density, ρ, and specific energy, $e = E - u^2/2$, of the homogeneous equilibrium fluid are needed. In the present work, these properties are calculated for ethylene using the Peng-Robinson equation of state (PR EoS) (Peng & Robinson 1976), with the three parameters including the critical temperature and pressure of 282.35 K and 5.0418 MPa and the acentric factor ω= 0. 087 (Reid et al. 2001).

Valve closure models

In the following, the effect of valve closure on the flow in the pipeline is described accounting for the type and closure characteristics of the isolation valve.

Automatic Shut-off and Remote Control Valves

For Automatic Shut-off Valves (ASV) and Remote Control Valves (RCV) , valve closure occurs during the time frame between the valve activation time, t_a and its complete closure time, t_c. In the case of ASV, t_a corresponds to the time when the fluid pressure drops below a set valve activation pressure threshold. Hence t_a depends on the fluid decompression wave velocity and the distance between the pipe failure location and the valve. For RCVs on the other hand, t_a is defined as the time for the valve activation by the operator following pipe failure. The valve closure time, t_c, can be simply expressed in terms of t_a and the valve linear closure rate, $\dot{z}_v$:

$$t_c = t_a + D/\dot{z}_v \quad (4)$$

During the ASV and RCV closure, their impact on the flow is modelled by introducing an additional pressure drop, Δp_v, at the valve location (Mahgerefteh et al. 1997):

$$\Delta p_v = \frac{1}{C_v^2}\frac{\rho u^2}{2} \quad (5)$$

where the C_v is the valve discharge coefficient. In the case of a ball valve, C_v may be expressed as a function of the valve opening area, A_v (Wylie & Streeter 1993):

$$C_v = \sum_{i=0}^{4} a_i \left(\frac{A_v}{A_o}\right)^i \quad (6)$$

where A_o is the nominal cross-sectional area of the pipe and a_i are fitting constants (a_0 = –0.00111888; a_1= 0.001104507; a_2 = 8.13 ·10^{-5}; a_3 = –1.73 ·10^{-6}; a_4 = 1.81 ·10^{-8}).

In equation (6), the valve opening area A_v may be evaluated at any time, t, during its closure using the following expression (Mahgerefteh et al. 1997):

$$A_v = \frac{4A_o}{\pi D} cos^{-1}\left(\frac{\dot{z}_v(t-t_a)}{2}\right) - \frac{\dot{z}_v t}{2}\sqrt{D^2 - \dot{z}_v(t-t_a)^2}. \quad (7)$$

In the present study, the closure rate for both ASVs and RCVs is assumed to be 2.54 cm/s, while the activation pressure threshold, Δp_a, for ASVs is set at 10 bar below the nominal operating pressure.

Check Valves

Check Valve (CV) closure time is characterised by the valve closure delay time, t_d spanning the period between the valve activation time, t_a upon the flow reversal, and its complete closure time , t_c. In the present study, the CV is assumed not to present any obstruction to the escaping fluid until its complete closure. Its subsequent impact on the flow is modelled by introducing a closed end boundary condition at the valve location.

Numerical solution

The numerical solution of the conservation equations (1) – (3), including the relevant closure correlations for the fluid physical properties, and valve boundary conditions, is obtained using the Method of Characteristics (Mahgerefteh et al. 1997; Mahgerefteh et al. 2016). To ensure convergence and stability, the pipeline is discretised uniformly into a large number of cells (10 m wide each), while the time integration step is chosen based on the Courant-Friedrich-Lewy criterion (Mahgerefteh et al. 2016).

Results and discussion

This section presents the results of simulation studies of the transient fluid flow behaviour upon the FBR of ethylene pipelines incorporating various types of emergency isolation valves.

The study is performed for a pipeline of 250 mm i.d. with wall thickness of 12 mm, representative of a typical ethylene onshore pipeline (Saville et al. 2004; EPS 2013; Ryder 1997). The pipe wall roughness is assumed to be 0.05 mm. The pipeline operating pressure and temperature prior to rupture are specified within the ranges relevant to operation of High-Pressure Ethylene Pipelines (HPEP) and Low-Pressure Ethylene Pipelines (LPEP) in various climates. Figure 1 shows the ethylene pressure-temperature phase diagram indicating the HPEP and LPEP operation envelopes (Saville et al. 2004). The nominal transportation velocity of the ethylene stream is assumed to be 1 m/s, typical for existing ethylene pipelines (IMPEL 2009; EPS 2013).

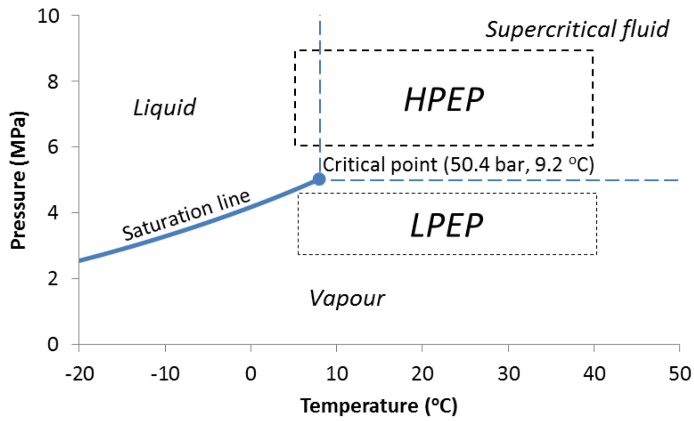

Figure 1. Pressure vs temperature phase diagram for ethylene with the HPEP and LPEP operation ranges.

In order to investigate emergency isolation efficacy of a pipeline incorporating the various types of ESDVs, the valve spacing is varied between 1 and 5 km, corresponding to those recommended for high consequence areas (DOT 2010).

Pressure surges

This part of the study is aimed at simulating the pressure surges induced in ethylene pipelines following the rapid closure of CVs in response to FBR failure.

Figure 2 shows schematically a section of a pipeline with FBR located at a distance x from the CV. In this study x is set to 300 m, while the distance L between the CV and pipe end is taken as 5 km, *i.e.* sufficiently long to ensure no interference of the decompression flow with the boundary conditions at the upstream and downstream ends of the pipe section.

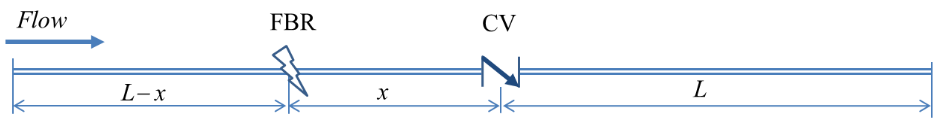

Figure 2. Section of a pipeline with a FBR upstream a check valve (CV).

Figure 3 shows an example of pressure history variation at the upstream side of CV (*i.e.* on the un-ruptured side of the pipe) for different valve closure times of 0.23,1.43,9.43 and 19.43 s. In all the cases the valve closure is accompanied by a compression shock, which strength decreases with the increase in the valve closure delay time. This can be explained by the decrease in the static pressure level at the valve as a result of the fluid decompression. While at closure delays of 0.23 s and 1.43 s the fluid pressure stays nearly unchanged after the passage of the shock, for the closure times longer than 9.43 s the pressure upstream of the valve gradually increases after passage of the shock during the pressure equilibration in the pipeline segment on the right of the valve (Figure 2).

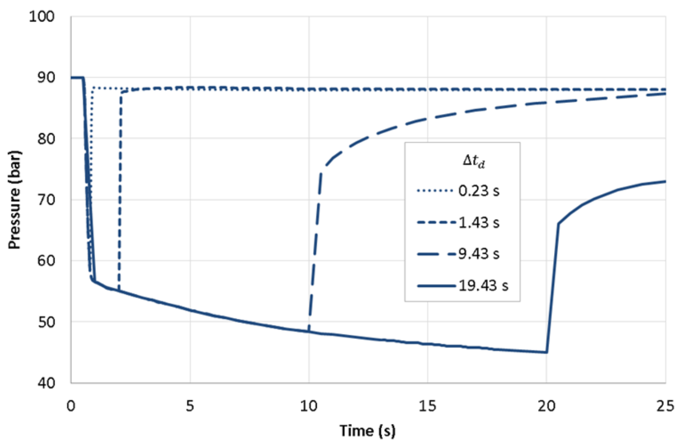

Figure 3. Pressure variation with time on the upstream side of CV activated following FBR of a pipeline transporting ethylene at 90 bar and 5 °C, as predicted for several different valve closure delay times, Δt_d.

Figures 4 *(a)* and *(b)* show the effect of the CV closure delay time on the pressure surge for pipelines operating at 30 – 90 bar pressures and temperatures of 5 and 30 ^oC, respectively. As the valve closure time increases, the pressure surge increases, with higher magnitude surges obtained at higher operating pressures. Remarkably, in the case where ethylene is transported in liquid phase at 90 bar and 5 ^oC (Figure 4, *a*), the surge pressure shows a large peak at the valve closure delay time of *ca* 2 s, while in all other cases studied, *i.e.* where the fluid is transported either in supercritical/liquid states at 60 and 90 bar or in vapour phase at 30 and 45 bar (see Figure 1), the surge pressure is relatively insensitive to the valve closure time, if it is greater than *ca* 4 s. Also, comparison of Figures 4 *(a)* and *(b)* shows that when transporting ethylene in vapour phase at 30 and 45 bar pressures, the fluid temperature has almost negligible effect on the surge pressure.

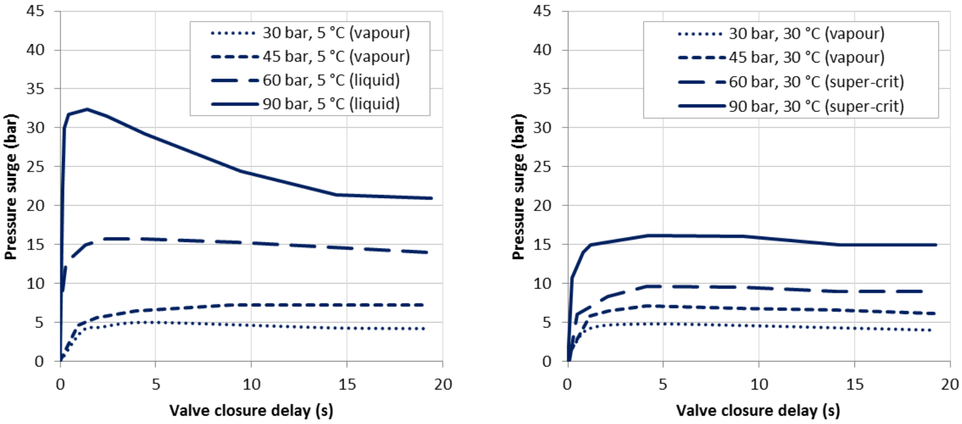

(a) *(b)*

Figure 4. Variation of the surge pressure with the closure delay time, as predicted at the upstream side of a CV for 250 mm internal diameter pipeline transporting ethylene at various initial pressures and initial temperatures of 5 ^oC *(a)* and 30 ^oC *(b)*.

In Figure 5, the effect of transportation temperature on the magnitude of the pressure surge is investigated at pipeline pressures of 90, 60 and 45 bar for a CV with the closure delay time Δt_d = 2 s. The results shown can be interpreted with the help of the Joukowsky equation for estimation of pressure surges for pipes carrying incompressible liquids (Muhlbauer 2004):

$$\Delta p = \rho u c_s, \quad (8)$$

where ρ and c_s are respectively the fluid density and speed of sound, and u is the flow velocity downstream the shock, corresponding to the fluid velocity prior to the valve closure.

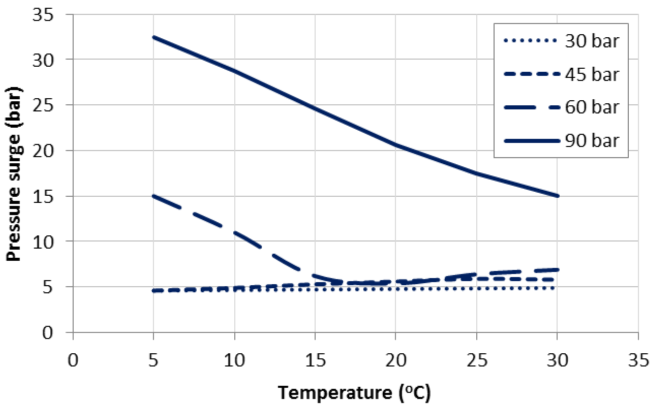

Figure 5. The effect of the ethylene pipeline temperature and pressure on the surge pressure on the upstream side of a CV with Δt_d = 2 s.

As follows from equation (8), the fluid density and speed of sound are the fluid properties affecting the surge pressure. In Figure 6 the product ρc_s is plotted as a function of temperature at pressures corresponding to Figure 5. Comparison of the data in Figures 5 and 6 shows that the pressures surge variations in Figure 5 has very similar trends to variation of ρc_s in Figure 6, explaining the observed in Figure 5 decrease in pressure surge magnitude with pressure at 90 bar and the increase in the surge pressure with pressure at low temperatures below *ca* 20 ^{o}C.

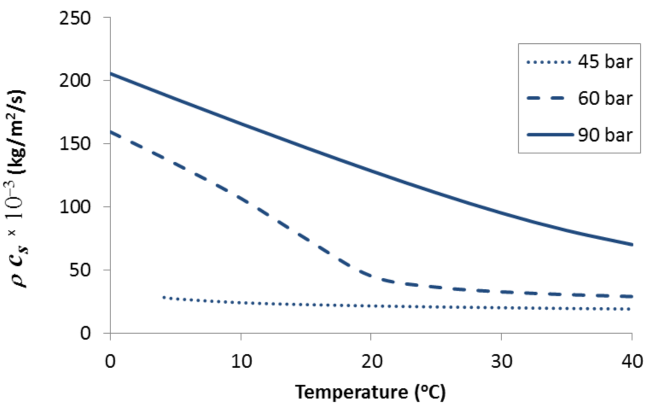

Figure 6. Variation of ρc_s with temperature at 45, 60 and 90 bar pressures for ethylene, as predicted using the Peng-Robinson EoS.

The pressure surges can create a thrust force acting on segments of the pipeline, potentially leading to deformations and vibrations in the pipeline. In order to prevent this, the pipeline support/anchoring blocks are commonly designed based on estimate of thrust load, F, caused by the surge pressure passing across the pipe bends (Antaki et al. 2005; Ord 2006):

$$F = \Delta p \cdot DLF \cdot A_o, \qquad (9)$$

where Δp is the pressure surge magnitude and DLF is the dynamic magnification factor, which is set to 2 at a maximum.

Using this equation, the thrust load created by 5 to 32 bar pressure surges in a 250 mm internal diameter pipeline (Figure 4) can be estimated to be in the range between *ca* 5 to 32 tonne. These forces are relatively large in comparison with the pipeline weight (*ca* 7 tonne for 100 m long section of 12 mm wall thickness 250 mm i.d. steel pipeline), indicating that surge protection measures should be carefully considered when using CVs in high-pressure ethylene pipelines.

Valve efficacy in minimising outflow following pipeline failure

In this section, the efficacy of emergency isolation using ASVs and RCVs is assessed by determining the amount of inventory escaping prior to complete isolation following FBR failure of a hypothetical high-pressure ethylene pipeline. The calculation of the amount of the released inventory is important, as such data serves as the source term for determining the consequences of pipeline failure, including fire, explosion or toxic release, ultimately dictating the minimum safe distances to populated areas and emergency response planning.

Figure 7 shows schematically a pipeline section with two ESDVs spaced at a distance L, and the FBR located at a distance x downstream the first valve (ESDV-1). Aiming to investigate the impact of FBR position on the pipeline emergency isolation, x is varied between 0 and L.

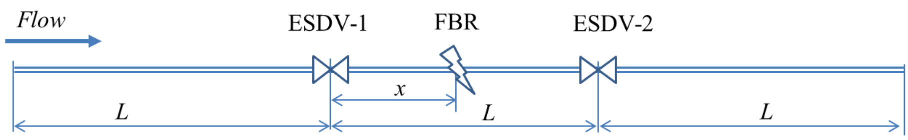

Figure 7. Position of two ESDVs and FBR along a pipeline.

Table 1. Types and characteristics of ESDVs setup on the pipeline (Figure 7).

Case No.	ESDV-1		ESDV-2	
	Valve type	Valve characteristics	Valve type	Valve characteristics
1	ASV	$\dot{z}_v$ = 2.54 cm/s, Δp_a = 10 bar	ASV	$\dot{z}_v$ = 2.54 cm/s, Δp_a = 10 bar
2	ASV	$\dot{z}_v$ = 2.54 cm/s, Δp_a = 10 bar	CV	Δt_d = 2 s
3	RCV	$\dot{z}_v$ = 2.54 cm/s, t_a = 240 s	RCV	$\dot{z}_v$ = 2.54 cm/s, t_a = 240 s
4	RCV	$\dot{z}_v$ = 2.54 cm/s, t_a = 240 s	CV	Δt_d = 2 s

To investigate the potential advantage of using CVs for emergency isolation in pipelines equipped with either ASV or RCV valves, four cases are simulated as listed in Table 1. In cases 1 and 3, ESDV-1 and ESDV-2 are of the same type, while in cases 2 and 4, CV is used as the downstream valve (ESDV-2).

The inventory mass loss, M_{loss} from a ruptured pipeline is given by:

$$M_{loss} = \int_0^{t_c} \dot{m}_{FBR} dt \; + \; A_o \int_0^L \rho(x, t_c) dx \qquad (10)$$

where the first term on the right hand side represents the cumulative mass released from the pipeline prior to complete valve closure. This is evaluated as an integral of the discharge flow rate, $\dot{m}_{FBR}$, predicted from the flow model. The second term on the right-hand side corresponds to the amount of inventory remaining in the isolated section of the pipe at the moment of complete closure of both valves.

The inventory loss calculated using equation (9) can be compared with the mass of fluid present in the pipeline isolated section prior to the rupture:

$$M_o = \rho_o \cdot A_o \cdot L \qquad (11)$$

where ρ_o is the fluid density at the pipeline transportation pressure and temperature.

Figure 8 shows the inventory losses predicted for cases 1 and 2 from Table 1 for the valve spacing distances, L of 1 and 5 km. As can be observed in Figure 8 *(a)* and *(b)*, the inventory losses predicted for the case 1 (*i.e.* when using solely ASV valves) are nearly the same for ruptures located close to either of the valves and attain minima at *ca* x/L =0.5. This can be explained by the fact that initial velocity of the flow in the pipe (1 m/s) is relatively small compared with the speed of the expansion wave propagating in the pipe. As such, the time of activation of the valve, and the resulting inventory losses are mainly affected by the distance between the valve and the rupture plane, but not the initial direction of the flow.

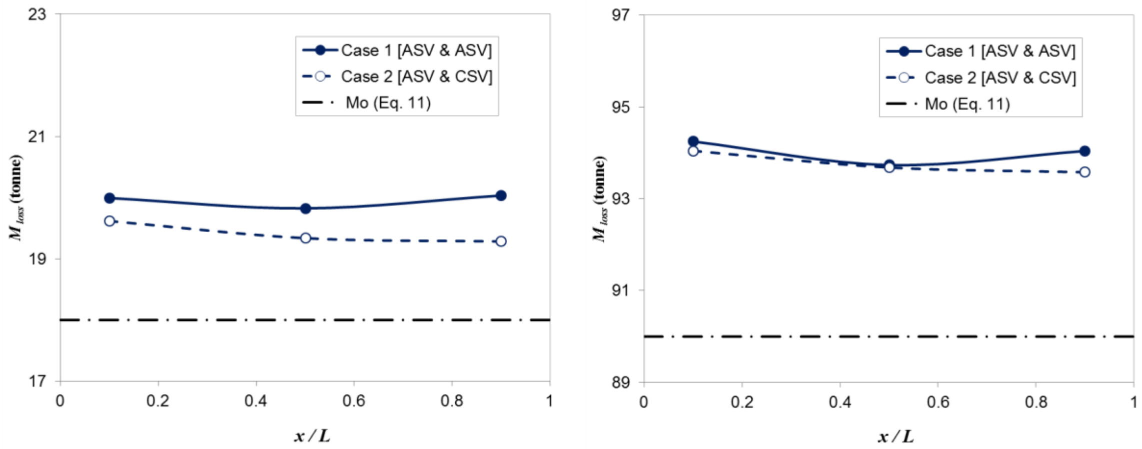

(a) *(b)*

Figure 8. Variation of the inventory losses a function of FBR position between ESDVs (Figure 7) in Cases 1 and 2 from Table 1, for the valve spacing L of 1 km *(a)* and 5 km *(b)*. The fluid in the pipeline is initially at 5 °C and 90 bar.

Figure 8 also shows that in contrast with the trend predicted for the case 1, M_{loss} predicted in the case 2 (*i.e.*, when using CV as the downstream isolation valve) progressively decrease with x/L. This can be explained by the fact that compared to

ASV, the CV enables faster isolation of the ruptured pipe segment when positioned closer to the rupture plane. However, the relative difference between the inventory losses between the cases 1 and 2 is less than 5%, meaning that CVs (setup in conjunction with ASVs), when compared with ASVs, offer no significant reduction in limiting the amount and the associated duration of the accidental release. In other words, apart from the safety factor, the additional factors of cost and reliability of emergency isolation system should be carefully considered when adding CVs to the pipelines equipped with ASVs.

Remarkably, M_{loss} data plotted in Figure 8, agree closely (within *ca* 10%) with the initial inventory M_o. The latter, as follows from equation (11), scales with the valve spacing distance, L. This indicates that ASVs with the closing rate of 2.54 cm/s (Table 1) enable relatively fast isolation of the pipeline segment.

Figure 9 shows the inventory losses, M_{loss}, predicted for the cases 3 (using RCVs) and the case 4 (using RCVs combined with CVs) for the emergency isolation (Table 1), for the 1 km and 5 km long valve spacing distance, L. In contrast with observations in Figure 8 where M_{loss} was found to scale with the valve spacing, in Figure 9, M_{loss} do not vary significantly with L. This can be explained by the relatively high rates of release, resulting in large amounts of fluid escaping from the pipeline by the time of the RCV activation at t_a = 240 s. Remarkably, due to the RCV finite response time, M_{loss} can still be significant even in the limit $L \to 0$.

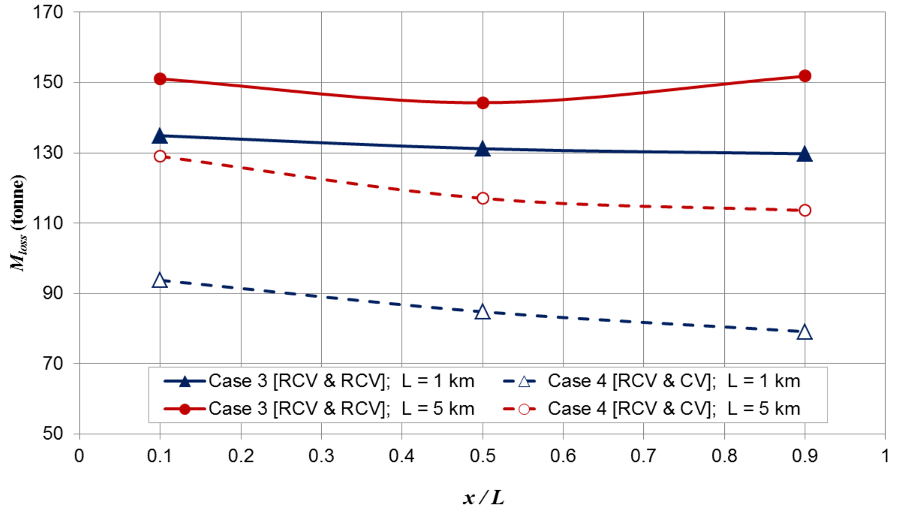

Figure 9. Variation of the inventory losses a function of position of FBR between the ESDVs (Figure 7) when using RCVs and RCV combined with CV (Table 1) for the valve spacing L of 1 km and 5 km. The fluid in the pipeline is initially at 5 °C and 90 bar.

Similar to what was discussed for the case 1 in Figure 8, the inventory loss curve obtained for the case 3 in Figure 9 is nearly symmetrical around x/L =0.5. Figure 9 also shows that combining RCV and CV (case 4, represented by dashed lines) offers significant reduction in the inventory losses as compared to emergency isolation based solely on RCVs (case 3, solid lines). This trend can be explained by significant delay in activation of RCVs as compared with CVs.

The above effect becomes more pronounced for shorter valve spacing distances L, as can be seen from comparison of the difference between the mass losses in the cases 3 and 4 predicted for L = 1 and 5 km at x/L = 0.1 (*i.e.* when the rupture is located close to the RCV). Indeed, at $x \to 0$ the mass losses from an isolated pipe section depend solely on the CV activation time that scales with the valve spacing distance, explaining the observed effect.

As such, the present study indicates that in pipelines with relatively short valves spacing, CVs setup in conjunction with RCVs or replacing RCVs at the downstream locations, can help to significantly reduce the amount of inventory escaping prior to complete pipeline isolation, and hence reduce the emergency isolation time for a ruptured section of the pipeline.

Conclusions

In this study, an established CFD model was employed to analyse the transient flow behaviour during emergency isolation following the full bore rupture of high-pressure pipelines transporting hazardous fluids. The objective was to use the data to enable the appropriate choice of ESDVs and spacing for effective mitigation of the accidental release. The study focused on ethylene transportation pipelines, given their extensive and growing use in the polymer manufacturing industry.

To analyse pressure surges accompanying closure of emergency check valves, a study was performed for wide range of ethylene pipeline operating pressures and temperatures. It was found that the pressure surge magnitude generally decreased with the operating pressure and temperature, varying non-linearly with the valve closure delay time. For ethylene pipelines operating at 90 bar pressure, the maximum amplitude of pressure surges is found to be *ca* 32 bar. This can lead to large thrust or bending forces acting on the pipeline segments, potentially damaging the pipeline. The CFD model applied in the present study enables accurate estimation of the pressure surges, as the key information for designing the pipeline anchoring and support structures.

In order to assess efficacy of emergency isolation valves, the amount of inventory released from an accidental rupture in a section between two ESDVs setup along a hypothetic pipeline was simulated. The results showed that addition of CVs to high-pressure ethylene pipelines equipped with ASVs does not affect significantly the duration of release. On the other hand, installing additional CVs in high-pressure ethylene pipelines equipped with RCVs, can significantly reduce the duration of release, hence assisting faster accident consequence mitigation. In practical cases, the benefits of using CVs should be traded against the safety, costs and reliability of operation of the emergency isolation scheme.

The present study also indicated that due to finite response time of RCVs, the duration of accidental release cannot be reduced below a threshold by using shorter valve spacing. This conclusion is practically important when deciding the maximum number of RCVs for emergency isolation of high-pressure pipelines.

The results of the present study lay the foundation for the future work on optimisation of ESDVs in long multi-segment pipelines transporting hazardous fluids.

Acknowledgement

This research was supported by Qatar National Research Fund (a member of The Qatar Foundation) NPRP award 8-1339-2-569. The authors are grateful to Wentian Zheng for his comments on the manuscript.

Nomenclature

A_o – pipe cross-sectional area, m^2;

A_v – valve opening area, m^2;

c_s – speed of sound, m/s;

C_v – valve discharge coefficient;

D – pipeline diameter, m;

e – specific energy, J/kg;

E – total specific energy, J/kg;

f_w – the Fanning friction factor;

L – valve spacing distance, m

M_{loss} – inventory mass loss, kg;

p – pressure, Pa;

t – time, s;

t_a – valve activation time, s;

t_c – valve closure time, s;

t_d – valve closure delay time, s;

u – velocity, m/s;

x – spatial coordinate, m;

$\dot{z}_v$ – valve linear closure rate, m/s.

Greek symbols:

Δp – pressure surge magnitude, Pa;

Δp_a – valve activation pressure threshold, Pa;

ρ – density, kg/ m^3.

References

Antaki, G.A. et al., 2005. *Guidelines for the Design of Buried Steel Pipe. Report by American Lifelines Alliance. ASCE and FEMA*, USA.

Chen, N.H., 1979. An Explicit Equation for Friction Factor in Pipe. *Industrial & Engineering Chemistry Fundamentals*, 18(3), pp.296–297.

CIA, 2017. Pipelines. *The World Factbook — Central Intelligence Agency*. Available at: https://www.cia.gov/library/publications/the-world-factbook/fields/2117.html

DNV, 2010. *Design and Operation of CO2 Pipelines, Recommended Practice*, DNV-RP-J202.

DOT, 2010. *192.179 Transmission line valves. Pipeline and Hazardous Materials Safety Administration*, USA.

DOT, 2012. *192.935 What additional preventive required to be reported as an incident and mitigative measures must an under part 191. operator take?. Pipeline and Hazardous Materials Safety Admin*, USA. Available at: https://www.gpo.gov/fdsys/granule/CFR-2011-title49-vol3/CFR-2011-title49-vol3-sec192-935.

EPPLP, 2017. Enterprise to Develop Ethylene Storage and Transportation Projects. Available at: https://www.businesswire.com/news/home/20170403005166/en/Enterprise-Develop-Ethylene-Storage-Transportation-Projects

EPS, 2013. EPS ethylene link starts up. *Pipeline Coating*. Available at: www.eps-pipeline.de.

Goodwin International Ltd, 2014. *Check Valves*, Stoke-on-Trent, UK. Available at: www.checkvalves.co.uk.

IMPEL, 2009. *Lessons learnt from industrial accidents. Seminar in Paris – France, 3-4 June 2009*, Available at: www.aria.developpement-durable.gouv.fr.

Koetzier, H., 1986. Dynamic Behaviour of Large Non-Return Valves. In *5th Int. Conf. on Pressure Surge*. Hanover, Germany, p. 213.

Mahgerefteh, H. et al., 2016. Modelling emergency isolation of carbon dioxide pipelines. *International Journal of Greenhouse Gas Control*, 44, pp.88–93.

Mahgerefteh, H., Saha, P. & Economou, I.G., 1997. A Study of the Dynamic Response of Emergency Shutdown Valves Following Full Bore Rupture of Gas Pipelines. *Trans IChemE Part B*, 75, pp.201–209.

Mahgerefteh, H., Saha, P. & Economou, I.G., 2000. Modeling fluid phase transition effects on dynamic behavior of ESDV. *AIChE Journal*, 46(5), pp.997–1006. Available at: http://dx.doi.org/10.1002/aic.690460512.

Muhlbauer, W.K., 2004. *Pipeline risk management manual. Ideas, Techniques, and Resources.* 3rd Ed. Elsevier, Oxford, UK.

Oland, C.. et al., 2012. *Studies for the Requirements of Automatic and Remotely Controlled Shutoff Valves on Hazardous Liquids and Natural Gas Pipelines with Respect to Public and Environmental Safety*, Report ORNL/TM-2012/411, Oak Ridge National Laboratory, Oak Ridge, Tennessee, USA. Avaialble at: http://www.osti.gov/bridge

Ord, S.C., 2006. Water Hammer – Do We Need To Protect Against It? How To Predict It and Prevent It Damaging Pipelines and Equipment. *Symposium Series No. 151*, (151), pp.1–20.

Papadakis, G.A., 1999. Major hazard pipelines: A comparative study of onshore transmission accidents. *Journal of Loss Prevention in the Process Industries*, 12(1), pp.91–107.

Peng, D.-Y. & Robinson, D.B., 1976. A New Two-Constant Equation of State. *Industrial & Engineering Chemistry Fundamentals*, 15(1), pp.59–64. Available at: http://pubs.acs.org/doi/abs/10.1021/i160057a011.

QNRF, 2014. Assessment of Hydrocarbon Transportation Pipelines. Qatar National Priority Research Progra. Project No. 8-1339-2-569.

Reid, R.C., Prausnitz, J.M. & Poling, B.E., 2001. *The Properties of Gases and Liquids* 5th ed., NY, USA: McGraw-Hill.

Ryder, A., 1997. *Environmental Impact Assessment in the Pipeline Industry. Experiences with the UK NW Ethylene Pipeline*. RSK/H/M03/35/06, RSK Environment Ltd. Helsby, UK.

S&P Global, 2012. Iran ethylene pipeline from Assaluyeh to Kermanshah to start Dec: report. Available at: http://www.platts.com/latest-news/petrochemicals/dubai/iran-ethylene-pipeline-from-assaluyeh-to-kermanshah-7228709

Saville, G., Richardson, S.M. & Barker, P., 2004. Leakage in Ethylene Pipelines. *Process Safety and Environmental Protection*, 82(1), pp.61–68. Available at: http://www.sciencedirect.com/science/article/pii/S0957582004711362.

Sulfredge, C.D., 2006. *Scoping Study on the Safety Impact of Valve Spacing in Natural Gas Pipelines*, Report ORNL/TM-2006/579, Oak Ridge National Laboratory, Oak Ridge, Tennessee, USA. Avaialble at: http://www.osti.gov/bridge

UK Gov & HSE, 1996. The Pipelines Safety Regulations. *UK Government Legislaiton*, (regulation 29), pp.1–8. Available at: http://www.hse.gov.uk/foi/internalops/hid_circs/enforcement/spcenf156.htm#annexa.

UKOPA, 2009. *UK Ethylene System*, UKOPA/09/0016. UKOPA Meeting, 25-26 February 2009. Available at: www.ukopa.co.uk/pdfs/UKOPA-09-0016.pdf

Vorozhtsov, A., Arkhipov, V. & Plekhanov, I., 2008. Emergency Shut-Down Valve for Gas Pipelines. *Strategic Insights*, VII(1), pp.1–3.

Woo, A., 2016. *Pipeline Integrity Valve Spacing Engineering Assessment (CDN) Leming Lake Sales Lateral NPS 16*, TransCanada Engineering Assessment, 28 July 2016. Available at: https://apps.neb-one.gc.ca/REGDOCS/File/Download/3013100

Wylie, E.B. & Streeter, V.L., 1993. *Fluid transients in systems*, the University of Michigan: Prentice Hall.